On the onset of the ridge structure in the framework of string percolation

A. Moscoso, C. Andrés and C. Pajares

Dept. of Particle Physics
University of Santiago de Compostela, Spain

International Conference on the Initial Stages in High-Energy Nuclear Collisions
September 12, 2013

Outline

Physical picture

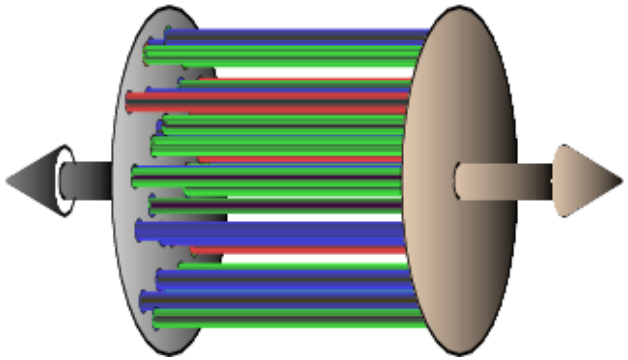

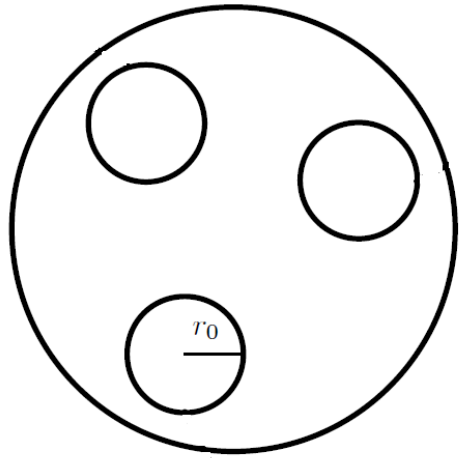

$r_0 = 0.2 - 0.25\ fm$

- Projectile and target interact via color field created by the constituent partons of the nuclei.
- Color field is confined in a region with transverse size $r_0 \sim \mathbf{0.2\,fm}$.
- We can see them as small areas in transverse plane.
- These color "strings" break producing $q\bar{q}$ pairs (Schwinger mechanism) that subsequently lead to the observed hadrons.

Physical picture

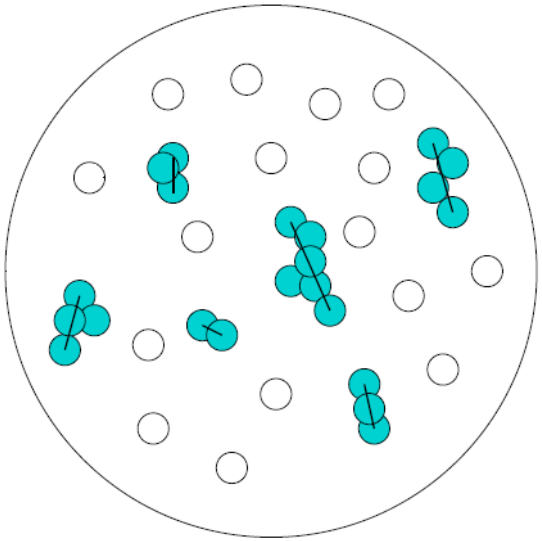

- With growing energy and/or atomic number of colliding particles, the number of **sources** grows $\rightarrow$ The **number of strings** grows with energy and/or atomic number.
- The **number of strings** also increases with increasing centrality.
- Strings are **randomly distributed** in transverse plane so they can overlap forming clusters.

String fusion

- A cluster of n strings **behaves like a single string with a color field**

$$\vec{Q}_n = \sum_1^n \vec{Q}_1$$

.

- The field is **randomly oriented** so

$$\left\langle \vec{Q}_n^2 \right\rangle = n \left\langle \vec{Q}_1^2 \right\rangle$$

- Using the Schwinger formula

$$\mu_n = \sqrt{\frac{nS_n}{S_1}}\mu_1 \,, \quad \left\langle p_T^2 \right\rangle_n = \sqrt{\frac{nS_1}{S_n}} \left\langle p_T^2 \right\rangle_1$$

where μ_n and $\left\langle p_T^2 \right\rangle_n$ are, respectively, the multiplicity and the mean p_T^2 of the particles created by the fragmentation of a cluster of n strings ocupping an area S_n.

Percolation

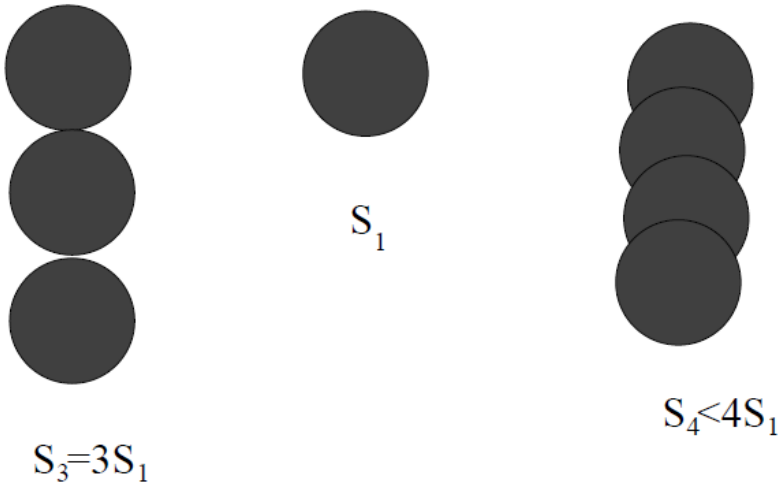

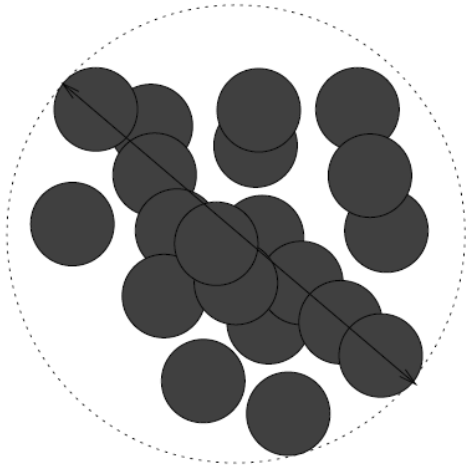

$$\eta = N_{st}\frac{S_1}{S_A}$$

- Limiting cases

$$\text{a)}\;\; S_n = nS_1 \longrightarrow \mu_n = n\mu_1\,, \quad \langle p_T^2 \rangle_n = \langle p_T^2 \rangle_1$$

$$\text{b)}\;\; S_n = S_1 \longrightarrow \mu_n = \sqrt{n}\mu_1\,, \quad \langle p_T^2 \rangle_n = \sqrt{n}\,\langle p_T^2 \rangle_1$$

- **At a certain critical density η_c ~1.2-1.5 a macroscopic cluster appears which marks the percolation transition.**

Average over cluster configurations

Homogeneous and high density case

- Mean fraction of the area covered by clusters

$$A(\eta) = 1 - e^{-\eta}$$

More realistic profile and also low density

- Mean fraction of the area covered by clusters

$$A(\eta) = \frac{1}{1 + ae^{-(\eta-b)/c}}$$

- So the basic equations concerning clusters are

$$\mu = N_s F(\eta)\mu_1\,, \quad \langle p_T^2 \rangle = \frac{\langle p_T^2 \rangle_1}{F(\eta)}, \quad \langle p_T^2 \rangle_1 \sim 1/r_0^2$$

$$F(\eta) = \sqrt{\frac{A(\eta)}{\eta}}$$

- $F(\eta)$ color reduction factor.

String percolation and CGC

- Transverse size

Percolation	CGC
$r_0^2 F(\eta)$	$1/Q_s^2$

- In the high density limit $\longrightarrow \sqrt{\eta} \sim Q_s^2$.
- Effective number of clusters $\longrightarrow$ flux tubes

$$\langle N \rangle = \frac{A(\eta) R_A^2}{r_0^2 F(\eta)} = A(\eta)^{1/2} \sqrt{\eta} \left(\frac{R_A}{r_0} \right)^2$$

In the high density limit $\longrightarrow \langle N \rangle = \sqrt{\eta} \left(\frac{R_A}{r_0} \right)^2$.

Percolation	CGC
$\langle N \rangle = \sqrt{\eta} \left(\frac{R_A}{r_0} \right)^2$	$\langle N \rangle = \frac{1}{\alpha_s} Q_s^2 R_A^2$

String percolation and CGC

- **Normalized 2-particle correlation function**

$$\mathfrak{R} \equiv \frac{\langle n^2 \rangle - \langle n \rangle^2 - \langle n \rangle}{\langle n \rangle^2} = \frac{\langle N^2 \rangle - \langle N \rangle^2}{\langle N \rangle^2} = \frac{1}{k}$$

  Low density limit: **n is basically Poisson-like** $\Longrightarrow k \to \infty$
  High density limit: $\langle N^2 \rangle - \langle N \rangle^2 \approx \langle N \rangle \Longrightarrow k \to \langle N \rangle \to \infty$

- These limits are satisfied by

$$k = \frac{\langle N \rangle}{A^{3/2}(\eta)}$$

Ridge structure

- Using the CGC result

$$\boxed{\frac{\Delta\rho}{\sqrt{\rho_{ref}}} = \Re\frac{dn}{dy}F(\phi)}$$

Percolation

$$\Re\frac{dn}{dy} = A(\eta)^{3/2}\mu_1$$

CGC

$$\Re\frac{dn}{dy} = \frac{1}{\alpha_s(Q_s)}$$

- Rapidity extension

$$\Delta y_{N_s} = \Delta y_1 + \frac{1}{2}\ln N_s/\langle N\rangle$$

$$= \Delta y_1 - \frac{1}{2}\ln F(\eta)$$

Results on 62 and 200 GeV Au-Au data from STAR

PHYSICAL REVIEW C **86**, 064902 (2012)

Anomalous centrality evolution of two-particle angular correlations from Au-Au collisions at $\sqrt{s_{NN}} = 62$ and 200 GeV

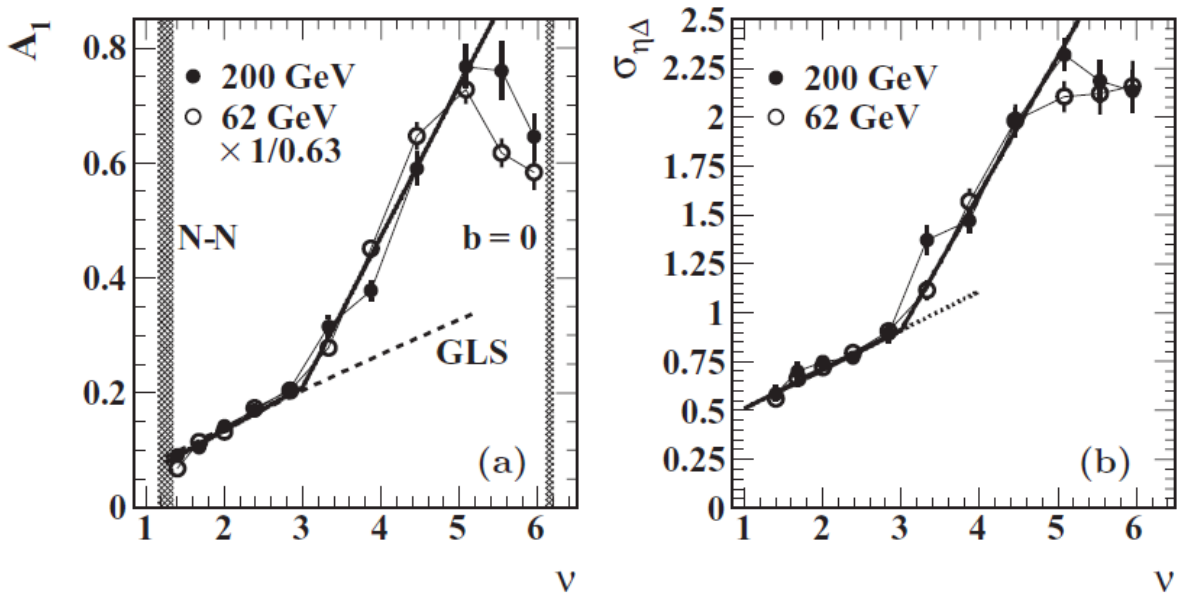

- Change in slope at $\nu \sim 3$ for both energies
- The corresponding densities are $\eta_{62} \sim 1.3$ and $\eta_{200} \sim 1.4$, **compatible with percolation transition**

Results on 62 and 200 GeV Au-Au data from STAR

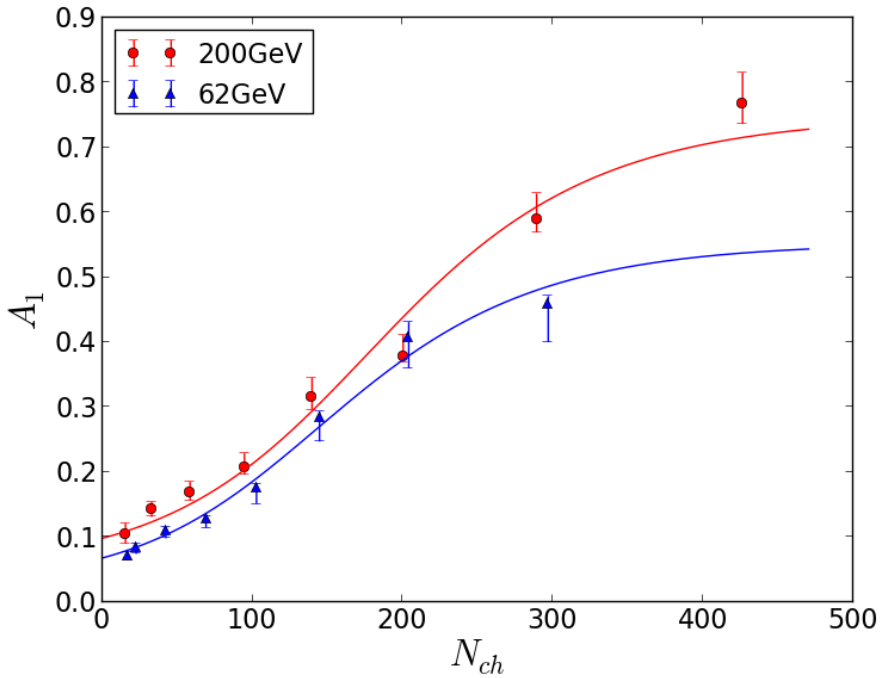

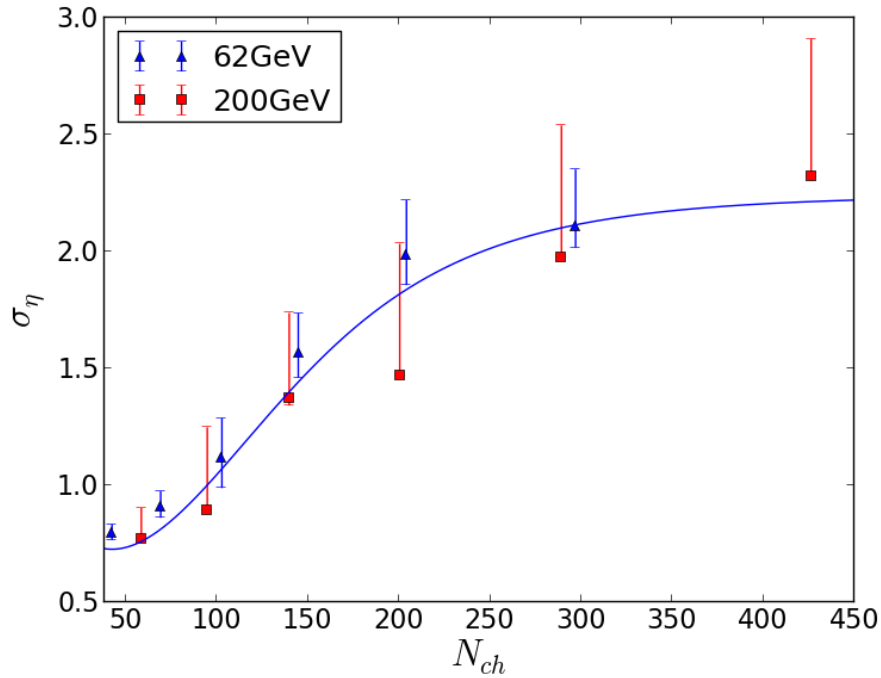

- $b \sim \eta_c \sim 1.4$

Qualitative prediction on 7 TeV p-p and 5.02 TeV p-Pb data from CMS

Physics Letters B 718 (2013) 795–814

Observation of long-range, near-side angular correlations in pPb collisions at the LHC ☆

CMS Collaboration *

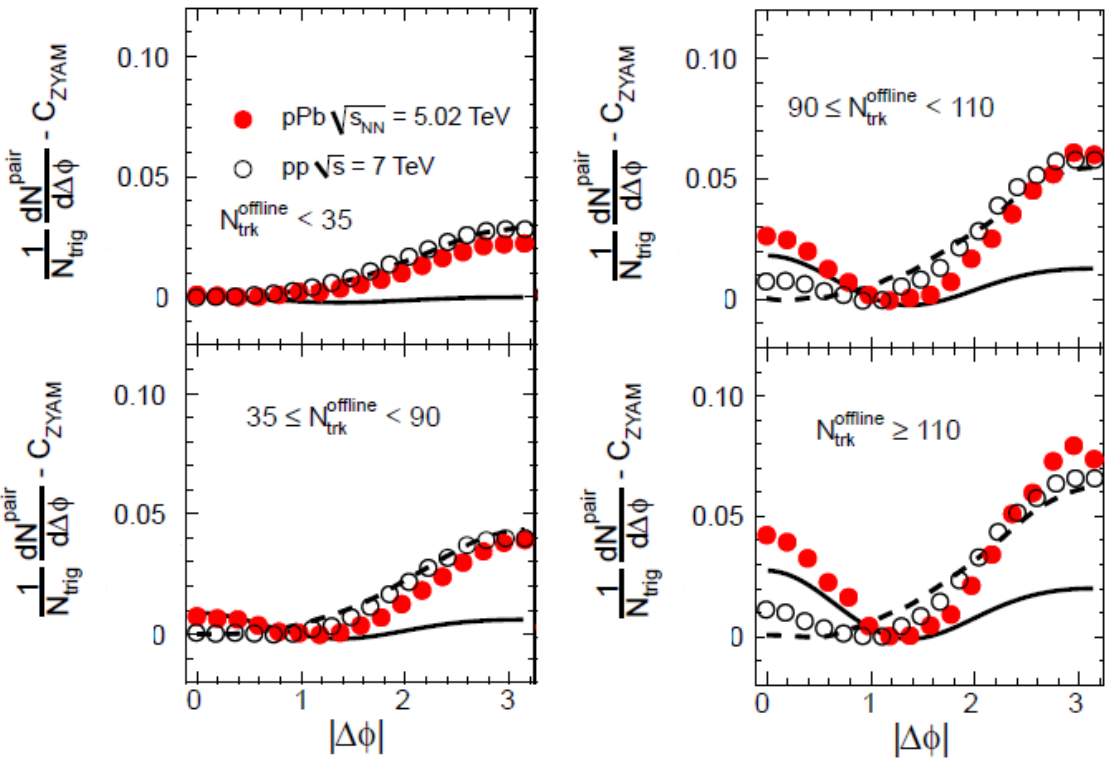

Qualitative prediction on 7 TeV p-p and 5.02 TeV p-Pb data from CMS

- For a 7 TeV pp collision with N_s ∼4-6 we expect N_{ch} ∼15-20

$$\eta \sim 0.25 - 0.35$$

- **Assuming an approximate proporcionality between η and N_{ch} the onset in protons is compatible with the percolation transition.**
- For pA (Dual Parton Model)

$$\frac{dn}{dy}_{pA} \approx \frac{1+\nu}{2}\frac{dn}{dy}_{pp} \sim 3\frac{dn}{dy}_{pp}$$

- **∼3 times less multiplicity than in pp is needed to reach the critical density.**

Summary

- Large similarities between CGC and percolation of strings. Similar predictions corresponding to similar physical picture. Percolation also explains the transition low density-high density.
- Quantitative agreement between Au-Au data from STAR and the prediction of percolation of strings.
- Onset of the ridge at least compatible with percolation transition for p-p and p-Pb data from CMS.

Extra Slides

Applicability of Monte Carlo Glauber models to relativistic heavy ion collision data

R L Ray and M S Daugherity
Department of Physics, The University of Texas at Austin, Austin, Texas 78712 USA
E-mail: ray@physics.utexas.edu

Au-Au 62 GeV

Centrality (%)	$\langle N_{ch} \rangle$	$\langle b \rangle$	$\langle N_{part} \rangle$	$\langle N_{bin} \rangle$	ν
90-100	2.4	$14.52^{+0.29(2.0)}_{-0.29(2.0)}$	$3.1^{+0.1(4.4)}_{-0.1(4.1)}$	$1.9^{+0.1(6.3)}_{-0.1(5.5)}$	$1.24^{+0.02(1.9)}_{-0.02(1.4)}$
80-90	6.6	$13.77^{+0.25(1.8)}_{-0.29(2.1)}$	$6.4^{+0.3(4.9)}_{-0.2(2.8)}$	$4.8^{+0.3(7.1)}_{-0.2(4.3)}$	$1.49^{+0.03(2.3)}_{-0.02(1.5)}$
70-80	14.6	$12.83^{+0.24(1.8)}_{-0.25(1.9)}$	$13.9^{+0.6(4.4)}_{-0.4(3.1)}$	$12.1^{+0.9(7.6)}_{-0.6(5.2)}$	$1.75^{+0.05(3.0)}_{-0.04(2.2)}$
60-70	29.0	$11.91^{+0.21(1.7)}_{-0.24(2.0)}$	$26.6^{+1.2(4.4)}_{-0.7(2.7)}$	$27.5^{+2.2(8.1)}_{-1.5(5.5)}$	$2.07^{+0.07(3.6)}_{-0.06(3.0)}$
50-60	52.3	$10.94^{+0.19(1.7)}_{-0.22(2.0)}$	$46.2^{+1.5(3.3)}_{-1.1(2.3)}$	$56.8^{+4.2(7.4)}_{-3.2(5.6)}$	$2.46^{+0.10(4.1)}_{-0.09(3.5)}$
40-50	87.1	$9.88^{+0.17(1.7)}_{-0.18(1.8)}$	$74.2^{+1.9(2.6)}_{-1.1(1.5)}$	$107.8^{+7.4(6.9)}_{-5.3(4.9)}$	$2.90^{+0.12(4.3)}_{-0.10(3.6)}$
30-40	136.9	$8.71^{+0.15(1.7)}_{-0.17(1.9)}$	$112.4^{+2.0(1.8)}_{-1.3(1.2)}$	$190.2^{+11.5(6.0)}_{-8.7(4.6)}$	$3.38^{+0.14(4.2)}_{-0.12(3.7)}$
20-30	205.5	$7.36^{+0.12(1.6)}_{-0.15(2.0)}$	$162.6^{+2.0(1.2)}_{-0.9(0.6)}$	$315.2^{+16.6(5.3)}_{-12.3(3.9)}$	$3.88^{+0.16(4.1)}_{-0.14(3.5)}$
10-20	300.7	$5.69^{+0.09(1.6)}_{-0.12(2.1)}$	$229.2^{+1.9(0.8)}_{-1.0(0.4)}$	$503.6^{+23.6(4.7)}_{-20.4(4.0)}$	$4.39^{+0.17(3.9)}_{-0.17(3.8)}$
5-10	395.5	$4.02^{+0.06(1.4)}_{-0.07(1.8)}$	$293.3^{+1.3(0.5)}_{-0.7(0.2)}$	$703.5^{+30.6(4.3)}_{-28.3(4.0)}$	$4.80^{+0.19(3.9)}_{-0.18(3.8)}$
0-5	480.8	$2.28^{+0.05(2.4)}_{-0.06(2.4)}$	$345.0^{+1.8(0.5)}_{-2.0(0.6)}$	$884.9^{+38.8(4.4)}_{-39.5(4.5)}$	$5.13^{+0.20(4.0)}_{-0.21(4.0)}$

Au-Au 200 GeV					
Centrality (%)	$\langle N_{ch} \rangle$	$\langle b \rangle$	$\langle N_{part} \rangle$	$\langle N_{bin} \rangle$	ν
90-100	2.9	$14.68^{+0.28(1.9)}_{-0.30(2.0)}$	$2.9^{+0.3(8.6)}_{-0.2(6.5)}$	$1.8^{+0.2(12.4)}_{-0.2(9.4)}$	$1.23^{+0.04(3.0)}_{-0.03(2.4)}$
80-90	8.2	$13.89^{+0.27(1.9)}_{-0.28(2.0)}$	$6.4^{+0.3(4.2)}_{-0.2(3.9)}$	$4.9^{+0.3(6.5)}_{-0.3(5.5)}$	$1.51^{+0.03(2.3)}_{-0.03(1.9)}$
70-80	18.7	$12.96^{+0.24(1.9)}_{-0.26(2.0)}$	$14.1^{+0.6(4.2)}_{-0.5(3.3)}$	$12.7^{+0.9(7.2)}_{-0.7(5.6)}$	$1.81^{+0.05(2.9)}_{-0.04(2.4)}$
60-70	37.8	$12.03^{+0.23(1.9)}_{-0.24(2.0)}$	$27.2^{+1.1(4.0)}_{-0.9(3.2)}$	$29.5^{+2.3(7.9)}_{-1.8(6.1)}$	$2.17^{+0.08(3.8)}_{-0.07(3.0)}$
50-60	69.7	$11.04^{+0.21(1.9)}_{-0.22(2.0)}$	$47.5^{+1.4(2.9)}_{-1.1(2.4)}$	$62.5^{+4.6(7.3)}_{-3.8(6.2)}$	$2.63^{+0.11(4.2)}_{-0.10(3.8)}$
40-50	118.5	$9.98^{+0.18(1.8)}_{-0.20(2.0)}$	$76.3^{+1.8(2.4)}_{-1.4(1.8)}$	$120.7^{+8.3(6.9)}_{-6.7(5.5)}$	$3.16^{+0.14(4.4)}_{-0.12(3.9)}$
30-40	190.2	$8.80^{+0.18(2.0)}_{-0.16(1.8)}$	$115.5^{+1.4(1.2)}_{-1.4(1.3)}$	$216.2^{+11.8(5.5)}_{-10.7(4.9)}$	$3.74^{+0.16(4.2)}_{-0.14(3.8)}$
20-30	291.5	$7.43^{+0.14(1.9)}_{-0.13(1.7)}$	$167.1^{+1.2(0.7)}_{-1.8(1.1)}$	$364.1^{+16.7(4.6)}_{-17.2(4.7)}$	$4.36^{+0.17(3.9)}_{-0.16(3.7)}$
10-20	433.5	$5.75^{+0.11(1.9)}_{-0.11(1.9)}$	$234.8^{+1.2(0.5)}_{-1.6(0.7)}$	$586.9^{+24.9(4.2)}_{-26.1(4.4)}$	$5.00^{+0.19(3.8)}_{-0.19(3.8)}$
5-10	577.6	$4.05^{+0.08(1.9)}_{-0.06(1.5)}$	$299.7^{+0.8(0.3)}_{-1.5(0.5)}$	$826.0^{+32.3(3.9)}_{-34.7(4.2)}$	$5.51^{+0.20(3.7)}_{-0.21(3.7)}$
0-5	705.6	$2.30^{+0.06(2.8)}_{-0.05(2.0)}$	$350.6^{+1.7(0.5)}_{-2.0(0.6)}$	$1043.6^{+43.2(4.1)}_{-44.1(4.2)}$	$5.95^{+0.23(3.8)}_{-0.23(3.8)}$